Attentional Bias for the Left Visual Field in Ambiguous Necker Cube Processing

Vladimir Maksimenko (maximenkovl@gmail.com)
Immanuel Kant Baltik Federal University
Alexander Kuc
Immanuel Kant Baltik Federal University
Artem Badarin
Immanuel Kant Baltik Federal University
Vadim Grubov
Immanuel Kant Baltik Federal University
Natalia Shusharina
Immanuel Kant Baltik Federal University
Alexander E. Hramov
Immanuel Kant Baltik Federal University

Research Article

Keywords: Attentional bias, ambiguous, Necker cube

Posted Date: March 18th, 2021

DOI: https://doi.org/10.21203/rs.3.rs-311162/v1

Attentional bias for the left visual field in ambiguous Necker cube processing

Vladimir Maksimenko[1,2,3], Alexander Kuc[1], Artem Badarin[1,2], Vadim Grubov[1,2,3], Natalia Shusharina[1], and Alexander E. Hramov[1,2,3]

[1]Immanuel Kant Baltik Federal University, Kaliningrad, Russia
[2]Neuroscience and Cognitive Technology Laboratory, Innopolis University, The Republic of Tatarstan, Russia
[3]Saratov State Medical University, Saratov, Russia.

ABSTRACT

There is a view that people better react to the stimuli presented in their left visual field (LVF) due to the right lateralization of the ventral attentional network (VAN). Previous studies used color-deviant stimuli and reported LVF bias for a bottom-up attentional component. Here we examined this effect for ambiguous stimuli, Necker cubes whose processing requires bottom-up and top-down attention. We instructed subjects to report cube's orientation, left or right, while manipulated their ambiguity. In line with other works, we suggested that ambiguity enhanced reliance on the top-down mechanisms. For low ambiguity, subjects responded faster to the left-oriented cubes. EEG power increased in the right temporoparietal junction (TPJ) for 0.3 s post-stimulus onset. For high ambiguity, we found no difference in response time and EEG power. These results may evidence VAN activation when processing the bottom-up stimulus features. The eye-tracking confirmed that subjects focused on the center of the stimulus. We hypothesized that they used peripheral vision to acquire sensory information. Therefore, the LVF attentional bias might influence the evidence accumulation process. Our results support the bottom-up attentional bias to the left visual field and provide evidence for the vital role of right TPJ in controlling bottom-up attention.

Introduction

Cortical and subcortical areas in the left hemisphere differ structurally and functionally from those in the right hemisphere. It causes lateralization of cognitive functions and affects behavioral performance. For instance, the fusiform face area is lateralized to the right hemisphere (RH)[1], Broca's area belongs to the left hemisphere (LH)[2]. Thus, subjects demonstrate LH dominance when processing words, whereas face processing induces RH dominance[3]. The motor functions are contralateral, defining better performance of the right hand than the left hand[4]. Finally, the attentional system exhibits hemispheric lateralization. There is a view that people better respond to the stimuli presented in their left visual field (LVF) due to the right lateralization of the attentional neural network[5]. The neuroimaging studies report that the attentional system includes the dorsal and ventral attentional networks[6]. The dorsal attention network (DAN) includes bilateral intraparietal sulcus and the frontal eye fields and subserves goal-directed, top-down processing[7]. The ventral attention network (VAN) comprises the temporoparietal junction and ventral frontal cortex and responds to relevant external environmental stimuli. The VAN is dominant in the right hemisphere and subserves bottom-up processing. In particular, VAN is activated when an unexpected event occurs and breaks one's attention from the current task[8].

To report an LVF attentional bias, Ref.[5] used color-deviant stimuli since they captured the bottom-up attention. This work will further support LVF bias during processing more complex stimuli requiring bottom-up and top-down attentional components. In this work, we considered an ambiguous stimulus, the Necker cube, which reflects a 2D drawing of a 3D cube[9]. The observer interprets this 2D image as the left- or right-oriented 3D cube depending on the edges' contrast[10,11]. For the particular contrast, a 2D image morphology does not contain distinctive features of a particular orientation, making it ambiguous.

We suppose that the observer defines the unambiguous orientation based on image morphology involving a bottom-up component. In contrast, to define the ambiguous orientation, they increase reliance on the top-down components such as expectations, or the context memory[12,13]. Thus, manipulating image ambiguity, one may change the impact of these two components.

Considering response times (RT), we found that high ambiguity increases RT, as reported in our earlier works on the Necker cube perception[14,15]. We also observed that for low ambiguity, subjects responded faster to the left-oriented than right-oriented stimuli. In contrast, when ambiguity was high, they took the same time to respond to different image orientations.

Testing EEG wavelet power, we found that unambiguous processing increased activation of the right-lateralized temporoparietal junction (TPJ) for 0.3 s post-stimulus onset, mainly for the right-oriented stimuli. In contrast, for high ambiguity,

we found no differences between the left-oriented and the right-oriented stimuli. These results may evidence VAN activation when processing the bottom-up stimulus morphology.

Finally, eye-tracking confirmed that subjects focused on the center of the stimulus. We hypothesized that they used peripheral vision to acquire sensory information. Therefore, the LVF attentional bias might influence the evidence accumulation process. Our results support the bottom-up attentional bias to the left visual field and provide evidence for the vital role of right TPJ in controlling bottom-up attention.

Materials and methods

Participants

Twenty healthy subjects (11 males and 9 females) aged from 26 to 35 with normal or corrected-to-normal visual acuity participated in the experiments. All of them provided written informed consent in advance. All participants were familiar with the experimental task and did not participate in similar experiments in the last six months. The experimental studies were performed under the Declaration of Helsinki and approved by the local Research Ethics Committee of the Innopolis University.

Visual stimuli

We chose an ambiguous 2D drawing of a Necker cube as a bistable visual stimulus[14,16–18]. A subject without perceptual abnormalities interprets this 2D image as a left- or right-oriented 3-D object. The ambiguity and orientation of the 3D cube depend on the balance between the brightness of the inner edges forming a left-lower ($b_l = 1 - a$) and right-upper ($b_r = a$) squares on the 2D image, $a \in [0,1]$ was a normalized edge's luminance in a gray-scale palette. Thus, the limit cases of $a = 0$ and $a = 1$ corresponded to unambiguous 2D projections of left- and right-oriented cubes, respectively, whereas $a = 0.5$ determined a completely ambiguous spatial orientation of the 3D cube.

In our experiment, we used a set of the Necker cube images with $a = \{0.15, 0.25, 0.4, 0.45, 0.55, 0.6, 0.75, 0.85\}$ (Fig. 1, A). On the one hand, this set could be separated into subsets of left-oriented (LO) $a = \{0.15, 0.25, 0.4, 0.45\}$ and right-oriented (RO) cubes $a = \{0.55, 0.6, 0.75, 0.85\}$. On the other hand, in accordance with our previous study[14], this set could be also divided into low-ambiguous (LA) images $a = \{0.15, 0.25, 0.75, 0.85\}$, which are easily interpreted by an observer, and high-ambiguous (HA) images $a = \{0.40, 0.45, 0.55, 0.60\}$, whose interpretations requires more effort. We also supposed that HA processing engages more top-down control.

Experimental procedure

We demonstrated Necker cubes (22.55 cm $\times$ 22.55 cm) on a white background using a 24" monitor (52.1 cm $\times$ 29.3 cm) with the 1920×1080 pixels resolution and 60 Hz refresh rate (Fig. 1, B). The distance between the subject and the monitor was $0.79 - 0.8$ m, and a visual angle was ~ 0.37 rad (Fig. 1, C). During the experiment, the subject was sitting in the "CE-1" chair (Neurobotics, Russia) specially approved for neurophysiological experiments. The monitor for stimuli presentation was placed on the table in front of the subject's eyes. We used the joystick to register the responses to stimuli — it was held by the subject's hands placed freely on the laps (see Fig. 1, C). The whole experiment lasted around 40 min for each participant, including short recordings of the eyes-open resting EEG state (≈ 150 s) before and after the main part of the experiment. During experimental sessions, the cubes with predefined values of a (chosen from the set in Fig. 1, A) were randomly demonstrated 400 times; each cube with a particular ambiguity was presented about 50 times.

We randomized parameter a in the following way. First, we formed a vector $A(1 \ldots 400)$, including all images (50 images for each value of a). Then, we randomized indexes in this vector by using the function *randperm* in MATLAB. It returned a row vector containing a random permutation of the indexes from 1 to 400 without repeating elements. Finally, this randomized vector of indexes determined the order of stimuli presentation. We randomized time of the stimuli presentations and pauses between them as $t_{min} + rand * (t_{max} - t_{min})$. Here, t_{max} and t_{min} defined minimal and maximal presentation/pause time, and *rand* is a MATLAB function that returns a single uniformly distributed random number in the interval (0,1).

Each i-th stimulus exhibition lasted for a time interval of τ and varied from $\tau_{min} = 1$ s to $\tau_{max} = 1.5$ s. Pauses, γ between the subsequent presentations of the Necker cube images contained the abstract picture exhibition and varied from $\gamma_{min} = 3$ s to $\gamma_{max} = 5$ s (Fig. 1, D). We instructed participants to press either the left or right key, responding to the left or the right stimulus orientation. We estimated a behavioral response for each stimulus by measuring the response time, RT, which corresponded to the time passed from the stimulus presentation to button pressing (Fig. 1, D).

The *first experiment* included EEG data registration. The EEG signals were recorded using the monopolar registration method and the classical extended 10–10 electrode scheme. We recorded 31 signals with two reference electrodes A1 and A2 on the earlobes and a ground electrode N just above the forehead. The signals were acquired via the cup adhesive Ag/AgCl electrodes placed on the "Tien–20" paste (Weaver and Company, Colorado, USA). Before the experiment, we used the abrasive "NuPrep" gel (Weaver and Company, Colorado, USA) to increase skin conductivity and reduce its resistance. After the electrodes were installed, the impedance was monitored throughout the experiments. Usually, the impedance values varied within a 2–5 kΩ

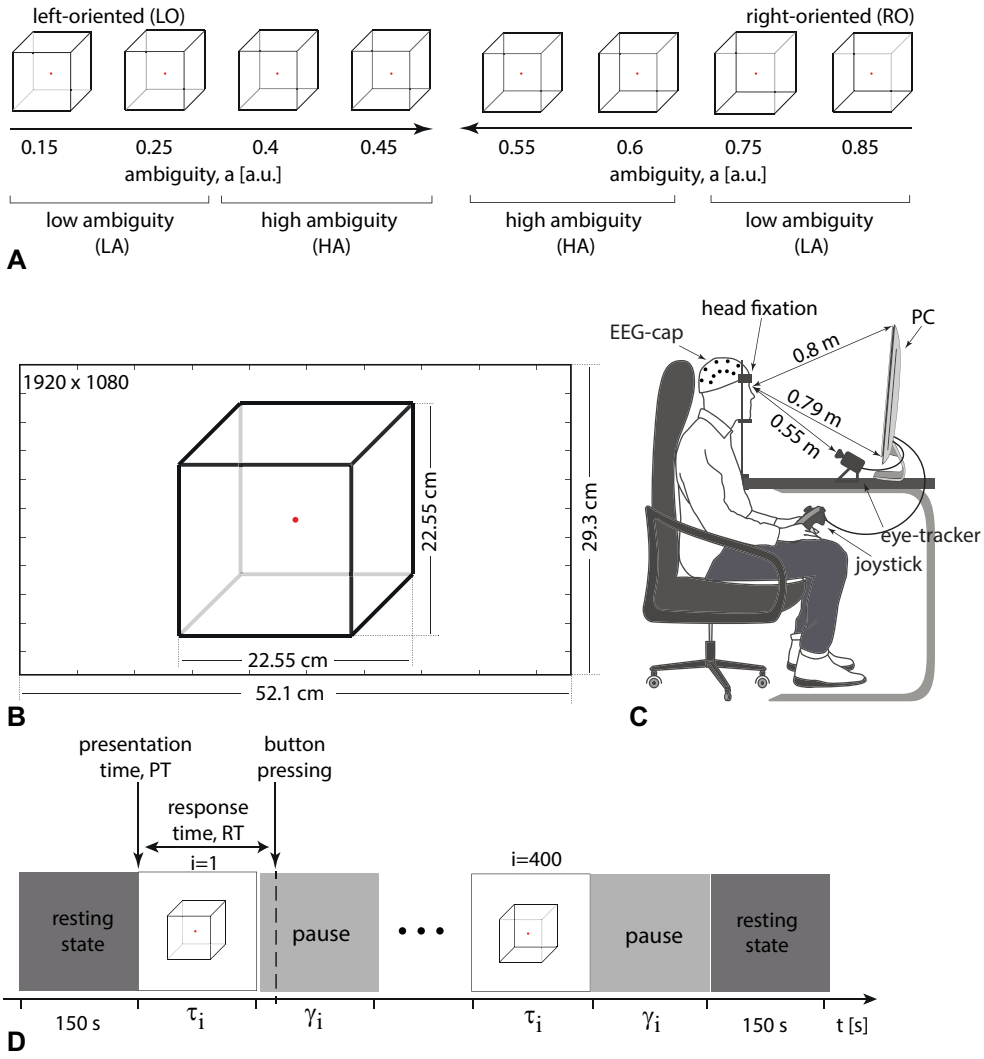

Figure 1. Visual stimuli A: the set of visual stimuli, Necker cubes, with different ambiguity a including high-ambiguity (HA), low-ambiguity (LA), left-oriented (LO), and right-oriented (RO) Necker cubes; B: example of the stimulus size on the screen; C: experimental environment; D: structure of the experimental session, τ_i is the duration of the i-th cube presentation, γ_i is the interval between the i-th and $(i+1)$-th presentations, RT is a response time.

interval. The electroencephalograph "Encephalan-EEG-19/26" (Medicom MTD company, Taganrog, Russian Federation) with multiple EEG channels and a two-button input device (joystick) was used for amplification and analog-to-digital conversion of the EEG signals. This device possessed the registration certificate of the Federal Service for Supervision in Health Care No. FCP 2007/00124 of 07.11.2014 and the European Certificate CE 538571 of the British Standards Institute (BSI). A band-pass FIR filter filtered the raw EEG signals with cut-off points at 1 Hz (HP) and 100 Hz (LP) and with a 50-Hz notch filter by embedded a hardware-software data acquisition complex. Eyes blinking and heartbeat artifacts were removed by Independent Component Analysis using EEGLAB software[19].

The *second experiment* tested the gaze direction data. It followed the design similar to the *first experiment* but included eye-tracking instead of EEG recording. We used eye-tracker EyeLink 1000 Plus (SR Research, Canada) with a high-speed camera to record eye-movement with a 1000 Hz rate. This configuration of the eye-tracker required head fixation for precise evaluation of gaze direction, so we used a special support device for the chin and forehead (see Fig. 1, C). The eye-to-monitor distance was the same as in the *first experiment* ($0.7-0.8$ m), and the eye-tracker was placed at the distance of 0.55 m. At the beginning of the experiment, we performed calibration individually for each subject to ensure the average error of gaze direction evaluation to be less than 0.3° (~ 15 pixels in monitor display coordinates). Only 9 subjects were available for the *second experiment*, so the data of these 9 subjects was used for gaze direction-based analysis (see section Eye-tracker data

analysis). The time interval between the two experiments was about 10 months.

EEG analysis

Similarly to Ref.[15], we divided EEG signals into trials. Each trial had a length of 4 s, and its middle point was time-locked to the stimulus onset. We calculated wavelet power (WP) in the frequency band of $1-40$ Hz using the Morlet wavelet for each trial. The number of cycles, n depended on the signal frequency, f, as $n = f$. To minimize between-subject variability, we considered normalized wavelet power (NWP) by contrasting WP on all trials to the WP averaged over 40-s baseline EEG before the experiment: $\mathrm{NWP} = (\mathrm{WP} - \mathrm{WP}_{baseline})/\mathrm{WP}_{baseline}$. All calculations were performed using the Fieldtrip toolbox in MATLAB[20].

Unlike the other works on ambiguous stimuli processing[21,22], we did not present completely ambiguous stimuli, such as a fully symmetrical cube with $a = 0.5$. Moreover, we instructed subjects to be as correct as possible. Therefore, we supposed that the subjects responded on the cube orientation based on the acquired sensory information, rather than the internal representations[12]. The subjects' overall correctness rates (CR) varied from 75.5% to 100% (M=95.1%, SD=6.4%). Based on the correctness rate, we excluded two subjects with CR of 75.5% and 80.0% as they exceeded the 90th percentile of CR distribution in the group. As a result, we proceeded with 18 subjects (M=97.07%, SD=2.6%). Finally, we excluded trials with the remaining high-amplitude artifacts and trials with erroneous responses. As a result, the number of trials varied from 148 to 253 (M=182, SD=30) in a group of subjects.

Source analysis

We estimated the source power in the frequency band of interest chosen based on the sensor-level analysis. We used the exact low-resolution brain electromagnetic tomography (eLORETA) to solve the inverse problem and reconstructed source activity from the EEG at each of the predefined points over brain volume[23–25]. "Colin27" brain MRI averaged template[26] was used to develop a boundary element method head model with three layers (brain, skull, and scalp)[27] and source space consisting of 11865 voxels inside the brain. We fitted the EEG electrodes' positions to the template head shape. First, we re-referenced EEG signals to the common average, demeaned them, and filtered by the fourth-order Butterworth bandpass filter with the passband f_L and f_H representing the frequencies of interest. Then, we performed time-lock averaging across the trials in each condition and computed the covariance matrix. Finally, we normalized the resulted source power P in each condition to the 40-s baseline EEG recorded at the beginning of the experiment as $(P - P_{baseline})/P_{baseline}$. To match the sources' locations with the brain's anatomical regions, we used the Automated Anatomical Labeling brain atlas[28]. All operations were performed using the Fieldtrip toolbox in MATLAB.

Eye-tracker data analysis

To analyze gaze direction, we considered monitor coordinates in pixels (x, y). We used all coordinates of gaze direction recorded during 0.5-second post-stimulus interval since it reflected the bottom-up processing. The distributions were constructed for x and y values separately with a bandwidth of ~ 15 pixels (average error of gaze direction evaluation) for each stimulus. We determined coordinates of each stimulus's fixation point (X,Y) as global maxima on x and y distributions. We then averaged these values over different types of cubes (left- and right-oriented LA, left- and right-oriented HA).

Statistical analysis

Statistical analysis followed a methodology, similar to our recent works[14,15]. We performed the group-level statistics for the median reaction time (RT) and presentation time (PT) with two within-subject factors: ambiguity and orientation. We also contrasted the number of the previously presented stimuli with four within-subject factors: current ambiguity, current orientation, previous ambiguity, previous orientation. The main effects were evaluated via repeated-measures ANOVA. The post hoc analysis used either paired samples t-test or Wilcoxon signed-rank test, depending on the samples' normality. Normality was tested via the Shapiro-Wilk test. We performed a statistical analysis using SPSS.

We analyzed NWP in the frequency band of $1-40$ Hz in two time-intervals of interest (TOI): TOI1 was a 1.5 s prestimulus interval; TOI2 was a 0.5 sec interval following the stimulus presentation; For TOI1, we averaged NWP over time and contrasted (channel-frequency) pairs between the conditions. For TOI2, we contrasted NWP for the (channel-frequency-time) triplets. To contrast the sensor-level NWP, we used paired t-test in conjunction with the nonparametric cluster-based correction for the multiple comparisons and the Monte-Carlo randomization. A cluster was significant when the p-value was below 0.025, corresponding to a false alarm rate of 0.05 in a two-tailed test. The number of permutations was 2000.

The source power was also contrasted via a paired t-test with the nonparametric cluster-based correction for the multiple comparisons. A cluster was significant when the p-value was below 0.025, corresponding to a false alarm rate of 0.05 in a two-tailed test. The number of permutations was 2000. We performed sensor-level and source-level statistical analysis in the Fieldtrip toolbox for MATLAB.

Table 1. Median Response time, RT [s] (ANOVA Summary)

Cases	dF1	dF2	Mean Square	F	p
Ambiguity (Low vs High)	1	17	.571	38.857	$< .001^*$
Orientation (Left vs Right)	1	17	.01	.827	.376
Ambiguity * Orientation	1	17	.038	16.397	$.001^*$

The gaze-direction was contrasted between the left- and right-oriented stimuli via a repeated-measures ANOVA with the fixation coordinate (X and Y) and stimulus orientation (left and right) served as the within-subject factors.

Results

Response times. We analyzed the median response time (RT) using a repeated-measures ANOVA with two within-subject factors: ambiguity and orientation (Table 1). As a result, we observed a significant main effect of the ambiguity and a significant interaction effect, ambiguity * orientation. The main effect of orientation was insignificant. Thus we concluded that subjects responded to the left- and right-oriented stimuli differently depending on the ambiguity. The post-hoc analysis revealed that the subjects responded faster to the LA stimuli than to HA ones (Fig. 2). When the ambiguity was high, RT to the left-oriented (M= 1.03 s, SD= .24 s) and right-oriented stimuli (M= 1.01 s, SD= .26 s) was similar: $t(17) = .67, p = .51$. (Fig. 2, A). In contrast, for low ambiguity, subjects responded faster to the left-oriented stimuli (M= .81 s, SD= .25 s) than to the right-oriented ones (M= .87 s, SD=.28 s): $t(17) = 3.31, p = .004$. (Fig. 2, B).

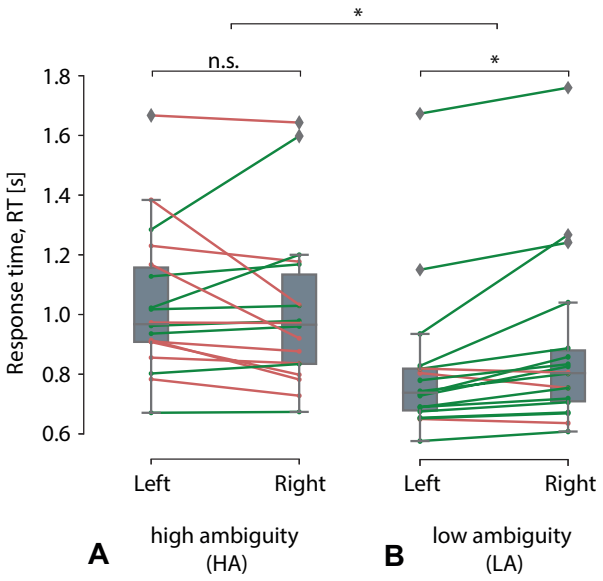

Figure 2. A result of RT comparison between the LO and RO stimuli The box-lot reflect median RT in the group of participants for the HA (A) and LA (B) stimuli. $^*p < .05$ via a repeated measures ANOVA and the post-hoc t-test.

According to our work[18], the repeated presentation of Necker cube images may induce a training effect resulting in the RT reduction. To ensure that the training did not affect the RT difference between LO and RO stimuli, we compared the median presentation times between the conditions. Table 2 provides evidence for the absence of PT bias between the conditions. Another work[15] suggests that RT to the Necker cube image depends on the previously perceived stimulus. Thus, RT to the right-oriented LA stimulus decreases if the previous stimulus has the same orientation. To ensure that the previous stimulus did not affect RT difference, we compared the number of the previously presented left-oriented and right-oriented with additional control for their ambiguity. Obtained results demonstrated no main effect of the previous stimulus orientation and no interaction effects of the previous orientation with other factors. Having summarized, we conclude that the RT difference between the left-oriented and right-oriented LA stimuli results from the difference in the stimuli's morphology.

Sensor- and source-level EEG wavelet power. Contrasting the sensor-level NWP between the left- and right-oriented LA stimuli during the prestimulus period, we found no significant clusters. Thus, we concluded that the observer's state remained

Table 2. Median Presentation time, PT [s] (ANOVA Summary)

Cases	dF1	dF2	Mean Square	F	p
Ambiguity (Low vs High)	1	17	3378.605	.535	.475
Orientation (Left vs Right)	1	17	4375.918	.945	.345
Ambiguity * Orientation	1	17	14849.432	1.131	.302

similar in these conditions. Contrasting NWP during the post-stimulus interval, we observed a significant negative cluster with $p = .042$ in the frequency band of $3-4$ Hz. This cluster appeared to form 0.23 s to 0.5 s post-stimulus onset (Fig. 3, A) and included EEG sensors in the right-lateralized occipital and parietal sensor lines (Fig. 3, B). The mean NWP in this cluster was higher when the subject processed the right-oriented stimulus than the left-oriented one (Fig. 3, C). Setting the time-frequency range based on the sensor-level analysis, we contrasted the brain activity on the source level. As a result, we observed a significant cluster with $p = .042$ including the right occipital, lingual, fusiform, supramarginal, and temporal gyri (Fig. 3, D).

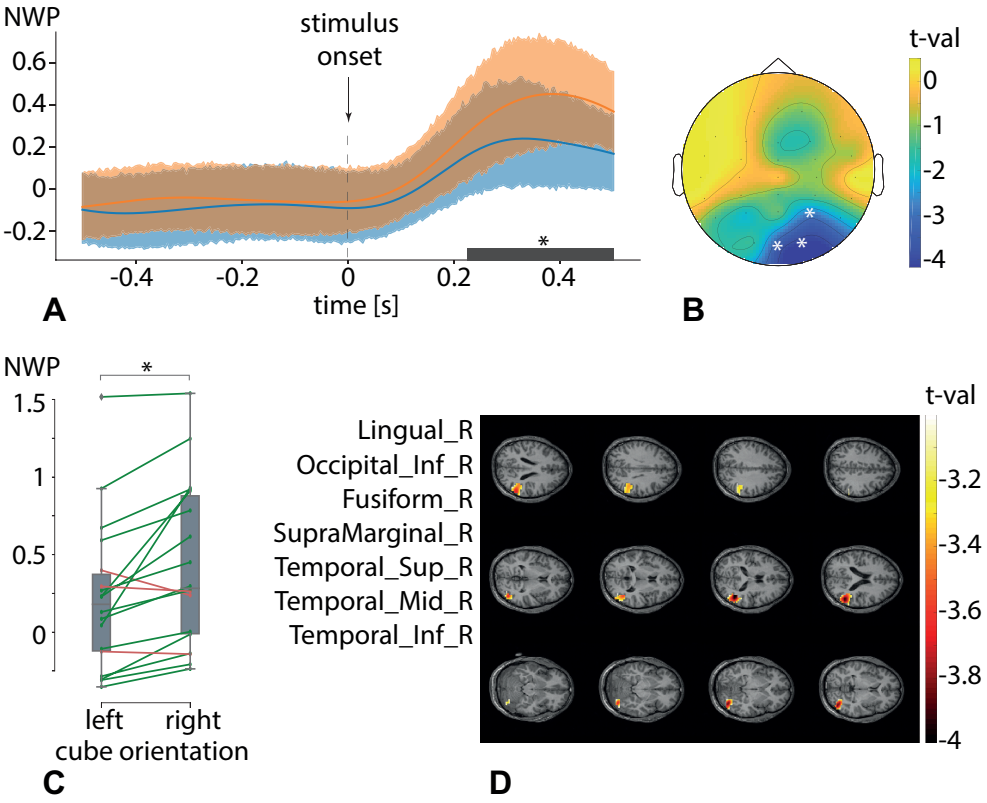

Figure 3. A result of NWP comparison between the LO and RO stimuli. The time-series (A) reflect the averaged NWP in the frequency band of $3-4$ Hz. The topogram (B) shows the averaged t-map and the right-lateralized channel cluster ($p_{pair} = .004, p_{cluster} = .042$). The box-plot (C) shows the mean NWP in this cluster for the LO and RO stimuli. The source-plot reflects t-value corresponding to the significant difference of the source power between the LO and RO stimuli ($p_{pair} = .005, p_{cluster} = .042$). All p-values are correct via a cluster-based test with the Montecarlo randomizations.

Gaze direction. The 9/18 subjects participated in the second experiment. It followed a similar design but included eye-tracking instead of EEG analysis. First, subjects' RTs to the LA stimuli were compared between these experiments. As a result, we observed a main effect of the orientation, while the effects of experiment and orientation*experiment were insignificant (see Table 3). Thus, we concluded that the RT bias between the left- and right-oriented LA stimuli presented in the second experiment. Contrasting the fixation point coordinates for the left- and right-oriented LA stimuli, we found no differences. A repeated-measures ANOVA revealed the main effect of coordinate reflecting differences of the monitor

Table 3. Median Response time to LA stimuli in two experimens, RT [s] (ANOVA Summary)

Cases	dF1	dF2	Mean Square	F	p
Experiment (1 vs 2)	1	8	.002	.033	.861
Orientation (Left vs Right)	1	8	.034	7.662	.024*
Experiement * Orientation	1	8	.006	2.109	.185

Table 4. fixation point to the left- and right-orientad LA stimuli (ANOVA Summary)

Cases	dF1	dF2	Mean Square	F	p
Orientation (left vs right)	1	8	195.983	.513	.494
dimension (X vs Y)	1	8	1.5×10^6	447.022	$< .001^*$
Orientation * Dimension	1	8	186.543	.684	.432

Table 5. fixation point vs the screen center (ANOVA Summary)

Cases	dF1	dF2	Mean Square	F	p
Location (fixation vs center)	1	8	1.2×10^4	2.994	.122
dimension (X vs Y)	1	8	1.5×10^6	447.022	$< .001^*$
Location * Dimension	1	8	2.051	.002	.963

horizontal and vertical dimensions (see Table 4). Finally, the fixation coordinated did not differ from the screen center (see Table 5). We concluded that subjects focused mostly on the center of the screen for the left- and right-oriented LA stimuli.

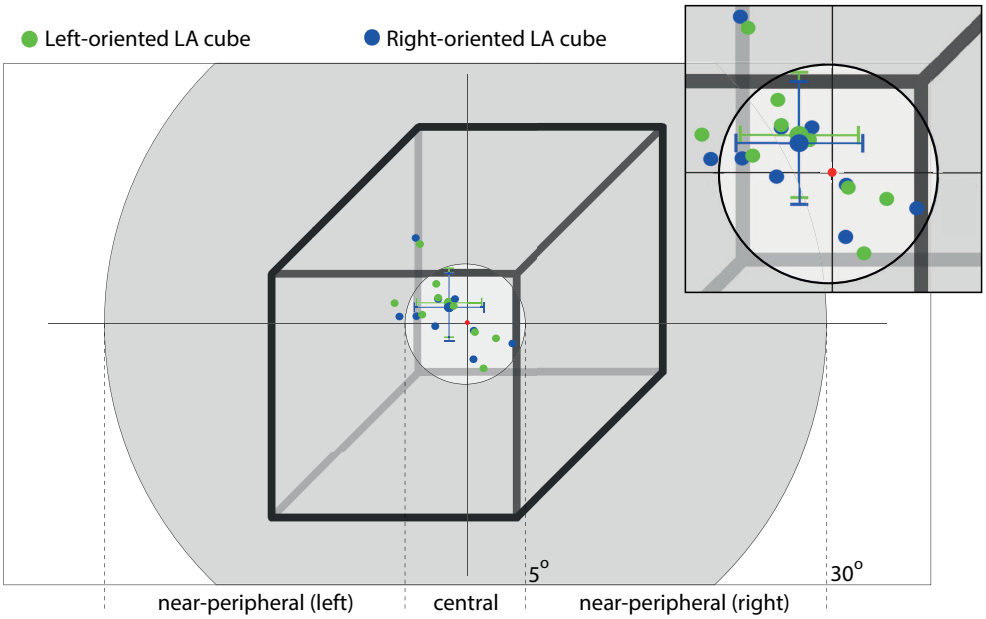

Figure 4. Gaze fixation. Green and blue dots reflect gaze fixation on the left- and right-oriented LA stimuli. Dots with whiskers show group mean and a standard deviation. The white and gray circles demonstrate the visual angles of 5° and 30° dividing central and peripheral vision.

Fig. 4 illustrates gaze fixation to the left- (green dots) and right- (blue dots) oriented LA stimuli. Dots with whiskers show group mean and a standard deviation. The red dot marks the screen center. The white and gray circles demonstrate the visual angles of 5° and 30° dividing central and peripheral vision. One can see, the stimulus appears in the areas of the central (white circle) and near-peripheral (grey circle) vision. In contrast, fixation points belong to the central rather than near-peripheral area

and remain similar for the left-oriented and right-oriented stimuli.

Discussion

We considered a perceptual decision-making task including ambiguous visual stimuli, Necker cubes. The participants responded to the stimulus orientation (left or right) using their left or right hand. Generally, high stimulus ambiguity increases the response time and probability of erroneous responses. Other studies suggested that wholly ambiguous stimuli have similar morphology, but their interpretation varies[29]. Similar morphology means that the bottom-up information stream barely provides decision-relevant features; therefore, decision mostly relies on the internal top-down processes such as memory and expectations[12,14,16].

We excluded the wholly ambiguous stimuli. As a result, the mean correctness rate exceeded 90%, manifesting reliance of the responses on the sensory information. Simultaneously, we also suggested that ambiguity increased the influence of top-down factors. When the ambiguity is low, the left- and right-oriented Necker cubes have different morphology. When ambiguity increases, all internal edges become equally visible; so, the left- and right-oriented Necker cubes worse differed. Our result showed that for low ambiguity, subjects responded faster to the left-oriented stimuli. In contrast, for high ambiguity, the response time hardly changed between the left-and right-oriented stimuli.

We hypothesized that the observed effect relied on the bottom-up mechanisms and diminished when the top-down processes dominated. Contrasting the prestimulus EEG power revealed no changes between left- and right-oriented stimuli. Thus, we supposed that changes in the observer state, including fatigue and motivation, barely caused changes in the response time. In the post-stimulus period, EEG power differed between the left- and right-oriented LA stimuli. We supposed that it reflected the various processing mechanisms caused by the morphological differences. For HA stimuli, where the morphology remained similar, no changes of EEG power were observed.

For LA stimuli, EEG power changed in the right-lateralized areas lying at the temporoparietal junction (TPJ), a part of the ventral attentional network. Literature suggests that VAN is lateralized to the right hemisphere and controls the bottom-up information processing[8]. Thus, activation of the right TPJ post-stimulus onset may indicate increased bottom-up attentional modulation. Fig. 3, A shows that EEG power in the right TPJ grows for both left- and right-oriented LA stimuli reflecting the processing of their morphological features. The right-oriented LA stimuli induced higher power in the right TPJ, evidencing increased bottom-up attention for this stimulus. These results suggest that the right-oriented LA stimulus has features that worse grab our bottom-up attention and require more demands.

A possible explanation is that the Necker cube has high spatial dimensions and covers both visual fields. The cube's morphology suggested that the sensory evidence for the left orientation appeared mostly in its left part. When visually examining stimulus from left to right, the observer starts seeing the internal edges that provide additional information about the right orientation. Another study described that subjects reported faster to the stimuli presented in the left visual field due to the right lateralization of VAN[5]. The eye-tracking data support this view. At the earlier processing stage (0.5 s. post-stimulus onset), subjects focused on the center of the left- and right-oriented stimuli. We hypothesized that they used peripheral vision to acquire sensory information. Therefore, the attentional bias to the left-visual field may affect the evidence accumulation process.

Recent work reported that hemispheric lateralization depends on the type of sensory information. Authors confirmed right hemisphere lateralization for face, global form, low spatial frequency processing, and spatial attention, and left hemisphere lateralization for visual word and local feature processing[3]. In our experiment, the sensory remains similar across conditions. Moreover, it is emotionally neutral and carries no semantic meaning. Thus, we suppose that right-lateralization is a marker of the attentional mechanism rather than information-specific processing.

Finally, we excluded the effect of motor preparation on the observed RT bias between the left- and right-oriented LA stimuli. First, we found a faster left-hand response in the right-handed participants, whereas a bulk of literature suggests the faster right-hand response (see Ref.[4] for the literature review). Second, motor preparation would affect RT regardless of the stimulus ambiguity.

Our results support the bottom-up attentional bias to the left visual field and provide evidence for the vital role of right TPJ in controlling bottom-up attention.

Acknowledgments

This work has been supported by the Russian Science Foundation (Grant 20-72-00036). Eye-tracker data analysis is supported by the President Program for Leading Russian Scientific School Support (NSh-2594.2020.2).

References

1. Jonas, J. *et al.* A face identity hallucination (palinopsia) generated by intracerebral stimulation of the face-selective right lateral fusiform cortex. *Cortex* **99**, 296–310 (2018).

2. Fedorenko, E. & Blank, I. A. Broca's area is not a natural kind. *Trends cognitive sciences* **24**, 270–284 (2020).
3. Brederoo, S. G. *et al.* Towards a unified understanding of lateralized vision: A large-scale study investigating principles governing patterns of lateralization using a heterogeneous sample. *cortex* **133**, 201–214 (2020).
4. Nisiyama, M. & Ribeiro-do Valle, L. Relative performance of the two hands in simple and choice reaction time tasks. *Braz. J. Med. Biol. Res.* **47**, 80–89 (2014).
5. Śmigasiewicz, K., Asanowicz, D., Westphal, N. & Verleger, R. Bias for the left visual field in rapid serial visual presentation: Effects of additional salient cues suggest a critical role of attention. *J. cognitive neuroscience* **27**, 266–279 (2014).
6. Vossel, S., Geng, J. J. & Fink, G. R. Dorsal and ventral attention systems: distinct neural circuits but collaborative roles. *The Neurosci.* **20**, 150–159 (2014).
7. Corbetta, M. & Shulman, G. L. Control of goal-directed and stimulus-driven attention in the brain. *Nat. reviews neuroscience* **3**, 201–215 (2002).
8. Farrant, K. & Uddin, L. Q. Asymmetric development of dorsal and ventral attention networks in the human brain. *Dev. cognitive neuroscience* **12**, 165–174 (2015).
9. Necker, L. A. Lxi. observations on some remarkable optical phænomena seen in switzerland; and on an optical phænomenon which occurs on viewing a figure of a crystal or geometrical solid. *The London, Edinburgh, Dublin Philos. Mag. J. Sci.* **1**, 329–337 (1832).
10. Kornmeier, J. & Bach, M. The necker cube—an ambiguous figure disambiguated in early visual processing. *Vis. research* **45**, 955–960 (2005).
11. Hramov, A. E. *et al.* Classifying the perceptual interpretations of a bistable image using eeg and artificial neural networks. *Front. neuroscience* **11**, 674 (2017).
12. Engel, A. K. & Fries, P. Beta-band oscillations—signalling the status quo? *Curr. opinion neurobiology* **20**, 156–165 (2010).
13. Scocchia, L., Valsecchi, M. & Triesch, J. Top-down influences on ambiguous perception: the role of stable and transient states of the observer. *Front. Hum. Neurosci.* **8**, 979 (2014).
14. Maksimenko, V. A. *et al.* Dissociating cognitive processes during ambiguous information processing in perceptual decision-making. *Front. Behav. Neurosci.* **14** (2020).
15. Maksimenko, V., Kuc, A., Frolov, N., Kurkin, S. & Hramov, A. Effect of repetition on the behavioral and neuronal responses to ambiguous necker cube images. *Sci. Reports* **11**, 1–13 (2021).
16. Wang, M., Arteaga, D. & He, B. J. Brain mechanisms for simple perception and bistable perception. *Proc. Natl. Acad. Sci.* **110**, E3350–E3359 (2013).
17. Kornmeier, J., Friedel, E., Wittmann, M. & Atmanspacher, H. Eeg correlates of cognitive time scales in the necker-zeno model for bistable perception. *Conscious. cognition* **53**, 136–150 (2017).
18. Maksimenko, V. A. *et al.* Neural interactions in a spatially-distributed cortical network during perceptual decision-making. *Front. behavioral neuroscience* **13**, 220 (2019).
19. Delorme, A. & Makeig, S. Eeglab: an open source toolbox for analysis of single-trial eeg dynamics including independent component analysis. *J. neuroscience methods* **134**, 9–21 (2004).
20. Oostenveld, R., Fries, P., Maris, E. & Schoffelen, J.-M. Fieldtrip: open source software for advanced analysis of meg, eeg, and invasive electrophysiological data. *Comput. intelligence neuroscience* **2011** (2011).
21. Kornmeier, J. & Bach, M. Bistable perception—along the processing chain from ambiguous visual input to a stable percept. *Int. J. Psychophysiol.* **62**, 345–349 (2006).
22. Yokota, Y., Minami, T., Naruse, Y. & Nakauchi, S. Neural processes in pseudo perceptual rivalry: An erp and time–frequency approach. *Neurosci.* **271**, 35–44 (2014).
23. Pascual-Marqui, R. D. Discrete, 3d distributed, linear imaging methods of electric neuronal activity. part 1: exact, zero error localization. *arXiv preprint arXiv:0710.3341* (2007).
24. Pascual-Marqui, R. D. *et al.* Exact low resolution brain electromagnetic tomography (eloreta). *Neuroimage* **31** (2006).
25. Pascual-Marqui, R. D. Theory of the eeg inverse problem. *Quant. EEG analysis: methods clinical applications* 121–140 (2009).

26. Holmes, C. J. *et al.* Enhancement of mr images using registration for signal averaging. *J. computer assisted tomography* **22**, 324–333 (1998).

27. Fuchs, M., Kastner, J., Wagner, M., Hawes, S. & Ebersole, J. S. A standardized boundary element method volume conductor model. *Clin. Neurophysiol.* **113**, 702–712 (2002).

28. Tzourio-Mazoyer, N. *et al.* Automated anatomical labeling of activations in spm using a macroscopic anatomical parcellation of the mni mri single-subject brain. *Neuroimage* **15**, 273–289 (2002).

29. Okazaki, M., Kaneko, Y., Yumoto, M. & Arima, K. Perceptual change in response to a bistable picture increases neuromagnetic beta-band activities. *Neurosci. research* **61**, 319–328 (2008).

Author contributions statement

AH and VM designed the study, AH and VM supervised the study, VG and AB conducted an experimental study, AK and NS performed the EEG data analysis, AK analyzed behavioral data, AB performed the eye-tracking data analysis, VM interpreted results, prepared illustrations and wrote the manuscript.

Additional information

Competing financial interests The authors declare that they have no competing interests.

Correspondence Correspondence and requests for materials should be addressed to VM (email: maximenkovl@gmail.com).

Figures

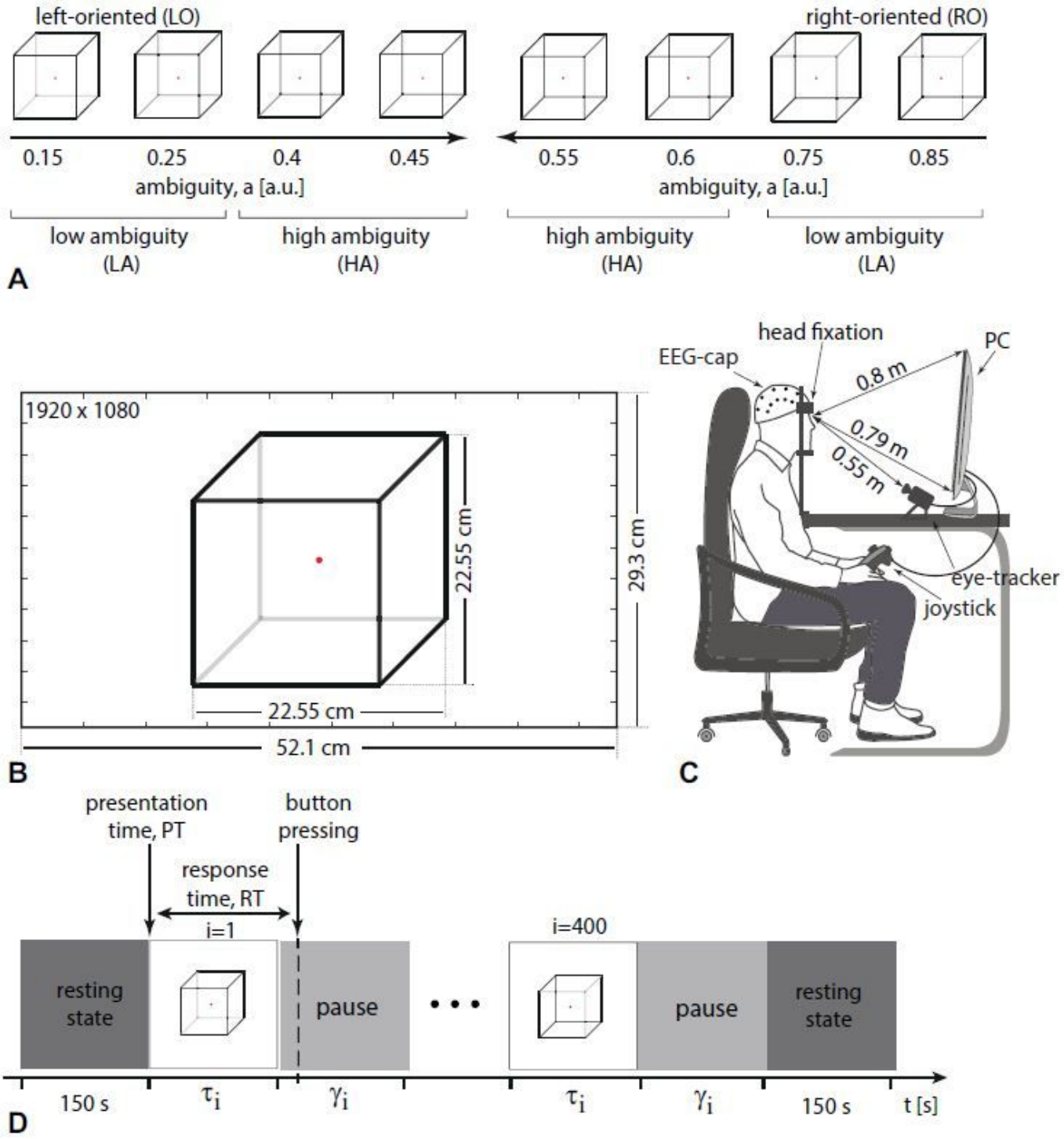

Figure 1

Visual stimuli A: the set of visual stimuli, Necker cubes, with different ambiguity a including high-ambiguity (HA), low-ambiguity (LA), left-oriented (LO), and right-oriented (RO) Necker cubes; B: example of the stimulus size on the screen; C: experimental environment; D: structure of the experimental session, τi

is the duration of the i-th cube presentation, γi is the interval between the i-th and (i+1)-th presentations, RT is a response time.

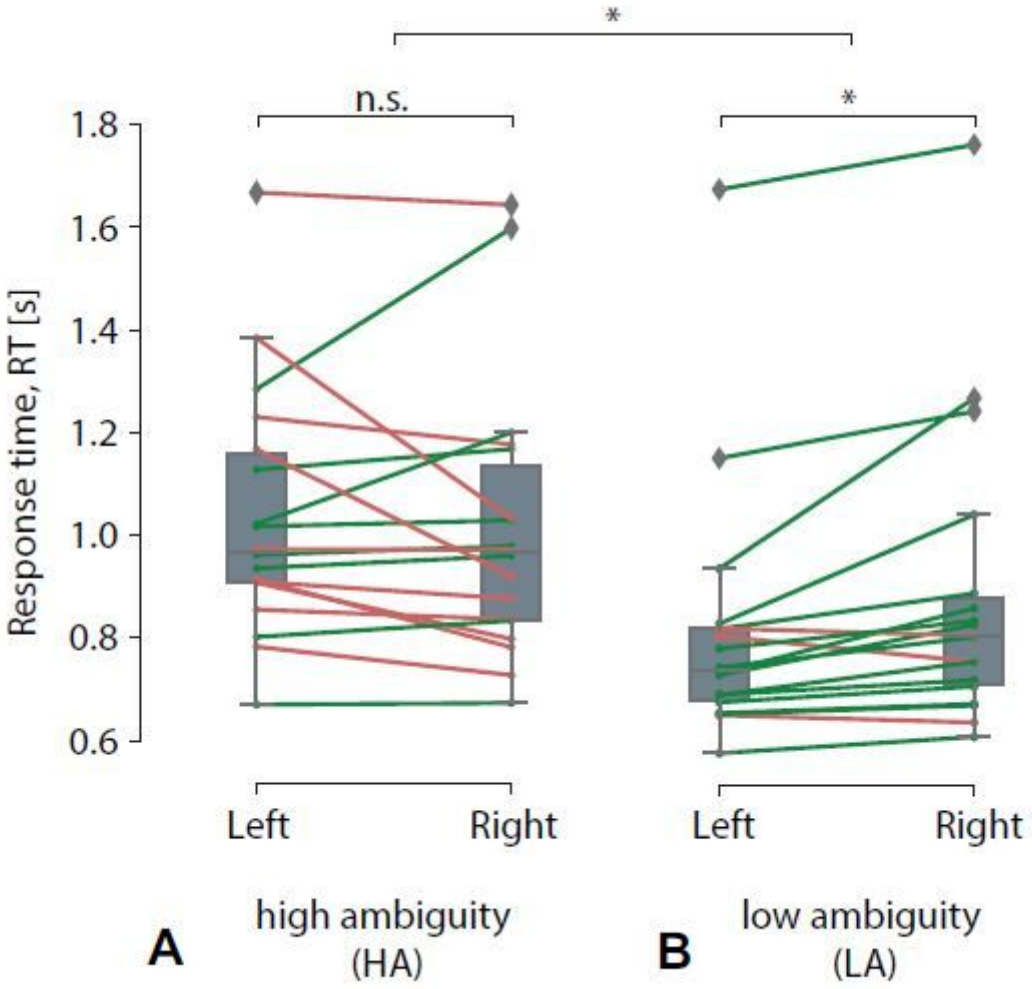

Figure 2

A result of RT comparison between the LO and RO stimuli The box-lot reflect median RT in the group of participants for the HA (A) and LA (B) stimuli. * p < :05 via a repeated measures ANOVA and the post-hoc t-test.

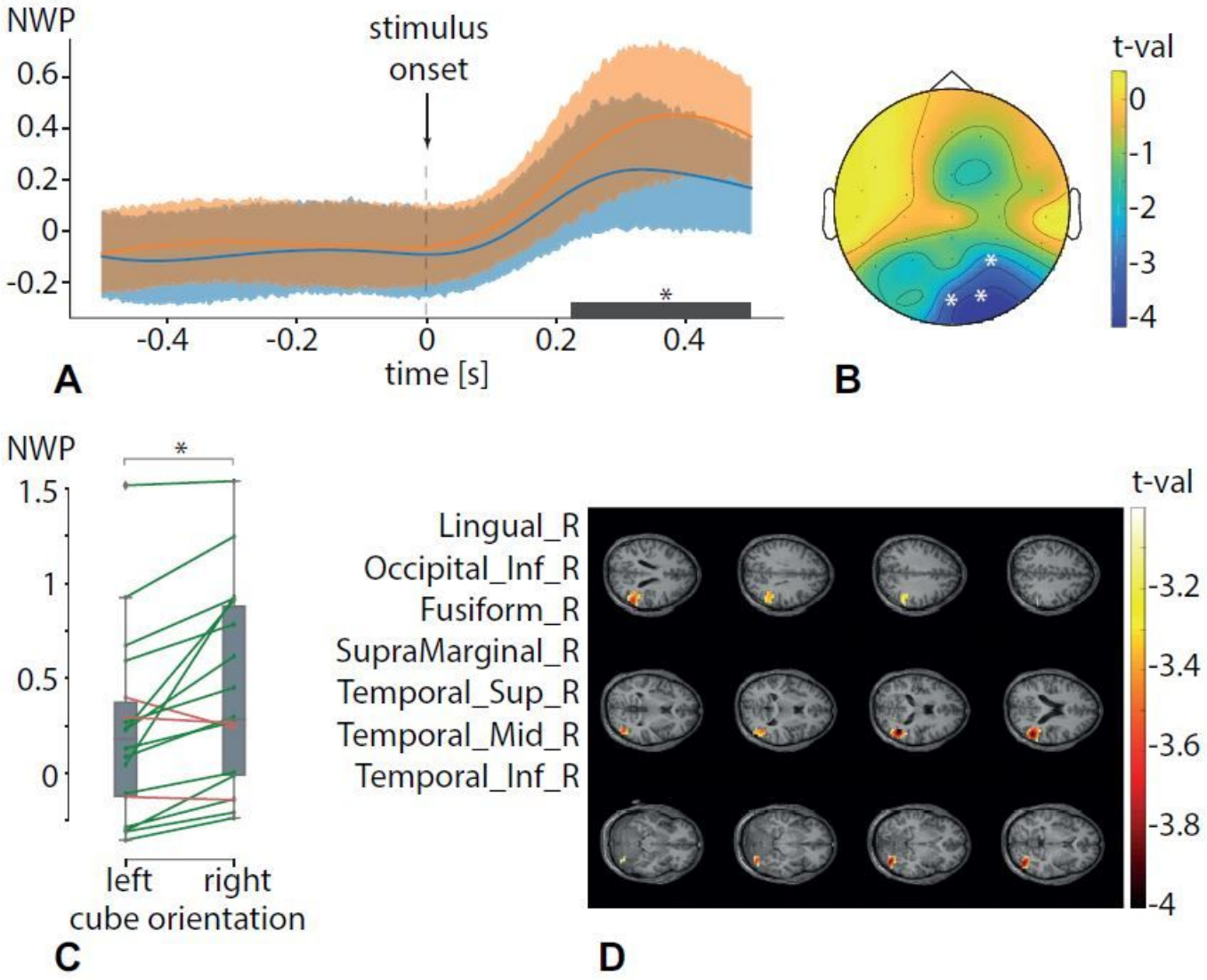

Figure 3

A result of NWP comparison between the LO and RO stimuli. The time-series (A) reflect the averaged NWP in the frequency band of 3 - 4 Hz. The topogram (B) shows the averaged t-map and the right-lateralized channel cluster (ppair = :004; pcluster = :042). The box-plot (C) shows the mean NWP in this cluster for the LO and RO stimuli. The source-plot reflects t-value corresponding to the significant difference of the source power between the LO and RO stimuli (ppair = :005; pcluster = :042). All p-values are correct via a cluster-based test with the Montecarlo randomizations.

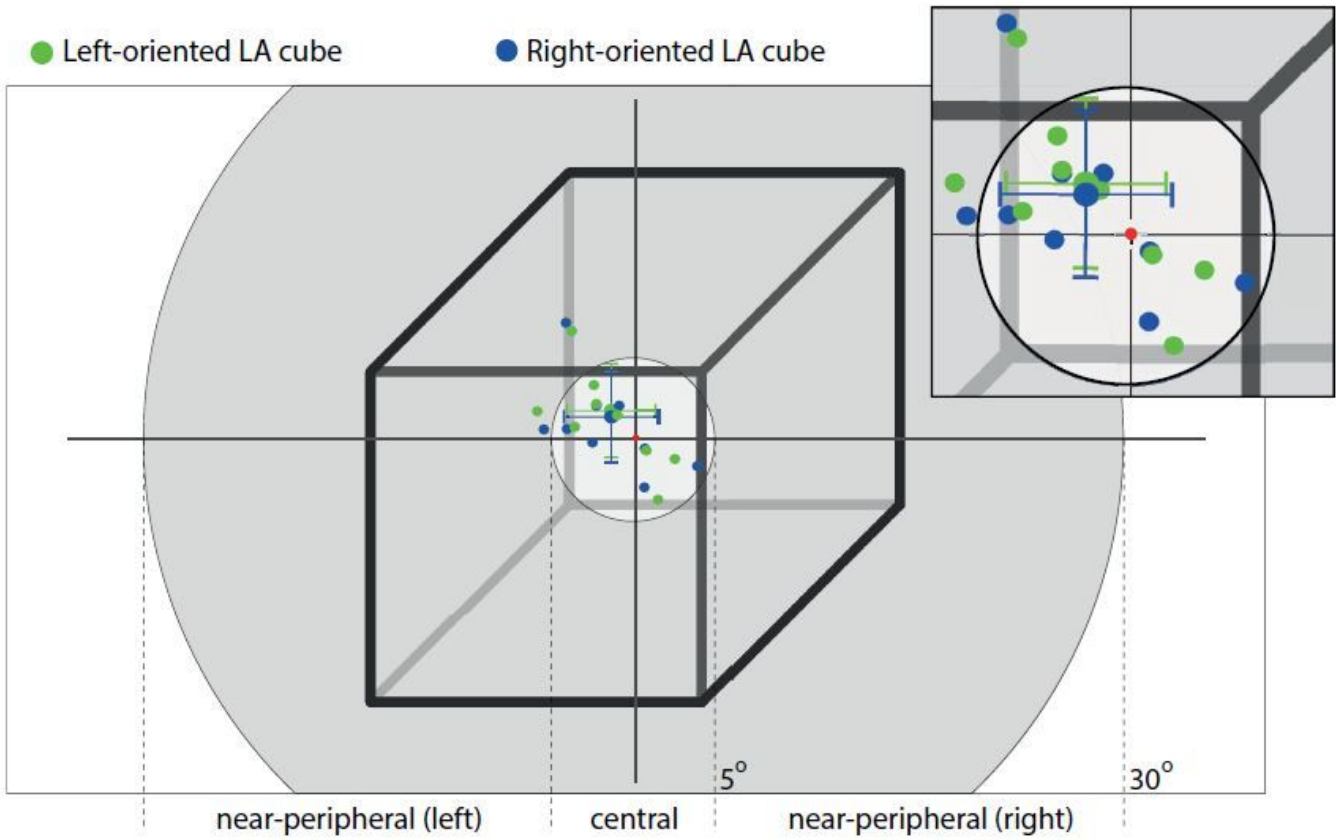

Figure 4

Gaze fixation. Green and blue dots reflect gaze fixation on the left- and right-oriented LA stimuli. Dots with whiskers show group mean and a standard deviation. The white and gray circles demonstrate the visual angles of 5° and 30° dividing central and peripheral vision.